Thermal stability and flame retardance of EVA containing DNA-modified clays

Thermal stability and flame retardance of EVA containing DNA-modified clays

Ewa Rajczak (Investigation) (Visualization) (Writing - original draft), Rossella Arrigo (Investigation), Giulio Malucelli (Conceptualization) (Supervision) (Writing - review and editing)

PII: S0040-6031(19)31098-6

DOI: https://doi.org/10.1016/j.tca.2020.178546

Reference: TCA 178546

To appear in: *Thermochimica Acta*

Received Date: 6 December 2019

Revised Date: 10 January 2020

Accepted Date: 3 February 2020

Please cite this article as: Rajczak E, Arrigo R, Malucelli G, Thermal stability and flame retardance of EVA containing DNA-modified clays, *Thermochimica Acta* (2020), doi: https://doi.org/10.1016/j.tca.2020.178546

Thermal stability and flame retardance of EVA containing DNA-modified clays

Ewa Rajczak, Rossella Arrigo, Giulio Malucelli*

Department of Applied Science and Technology, and local INSTM Unit, Viale Teresa Michel 5, 15121 Alessandria (Italy)

* corresponding author: e-mail: giulio.malucelli@polito.it

Graphical abstract

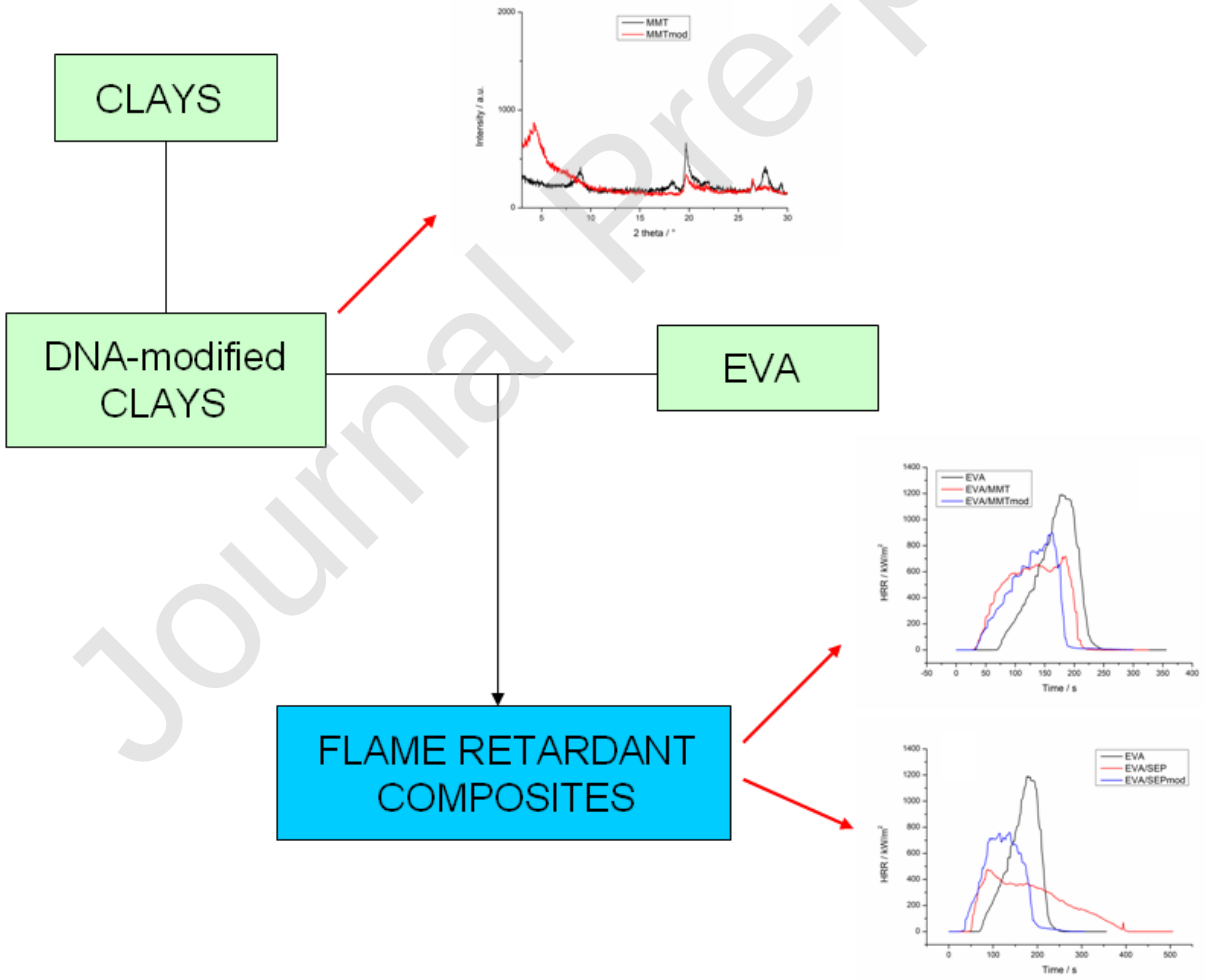

Highlights

- DNA-modified clays were embedded at 10 wt.% loading in EVA copolymer;
- New formulations increased the stiffness of the polymer matrix;
- Observed decrease in the peak of heat release rate and thermal parameters;
- Registered suppression in total smoke production and other smoke parameters.

Abstract

In this paper, two natural clays (namely, Sodium Cloisite and Sepiolite) were modified with low MW DNA from herring sperm and compounded in EVA copolymer (19% of vinyl acetate) at 10 wt.% loading, using an internal mixer. The effect of the presence of the biomacromolecule-modified fillers on the thermal properties and on the flame retardance of the resulting composites was thoroughly investigated. In particular, thermogravimetric analyses showed that the presence of the DNA-modified filler enhanced the thermal and thermo-oxidative stability of the polymer matrix. Despite a very limited effect on flammability, cone calorimetry tests revealed that the DNA-modified nanofillers were able to significantly decrease the heat release rate, the peak of heat release rate, the total smoke production, and the specific extinction area. Finally, the presence of the modified nanofillers was responsible for the increase of stiffness, as well as for a certain decrease of ductility of the polymer matrix, as assessed by tensile tests.

Keywords: EVA copolymer; Nanoclays; DNA; thermal stability; flame retardance.

1 Introduction

Thermoplastics and thermoplastic-based nanocomposites are widely used in industry and have found a broad number of engineered applications, ranging from automotive, aeronautical, electronics, packaging, construction, up to the biomedical sector [1–5]. However, if not inherently flame retarded, they cannot be exploited for many advances uses, for which the resistance to a flame application or to the exposure to an irradiative heat flux is mandatory. Therefore, improving the fire retardant properties of thermoplastic systems is always a challenging issue. In this regard, EVA (ethylene-*co*-vinyl acetate) is a thermoplastic widely employed; some of its applications deal with the coating of electrical wires and cables. However, its main disadvantage is connected with high flammability and

emission of great amounts of smoke while burning [6]. A common approach to fix this issue is to embed some flame retardant (FR) additives in the copolymer matrix, having different structures, fire retardant mechanisms and fire performances as well. As a result, very often, the good fire performances achieved in the resulting flame retardant copolymer are accompanied by significant changes in its mechanical behavior (i.e. stiffness, ductility and toughness) [7]. EVA copolymers are compounded with inorganic hydroxides, like magnesium hydroxide or aluminum trihydrate; however, usually loadings beyond 50 wt.% are required to get satisfying flame retardant performances [8,9]: as a consequence, the filled copolymers usually show poor mechanical properties, as they become stiffer but, at the same time, very brittle.

As clearly reported in the literature, one possibility to overcome this issue is to incorporate fillers at the nanoscale, such as nanoclays: they are able to create a ceramic physical barrier on the surface of the degrading material during a combustion process, hence lowering the heat and mass transfer from the material to the surroundings and vice-versa [10–12]. Thus, this approach allows decreasing the flame retardant loadings below 15 wt.%, even, in some cases, beneath 5 wt.% [13–16]. Two of commonly known clays are montmorillonite (MMT; general formula: $(Na,Ca)(Al,Mg)_6(Si_4O_{10})_3(OH)_6$-$n$$H_2O$) [17] and soft white fibrous sepiolite (SEP; general formula: $Mg_8Si_{12}O_{30}(OH)_4(H_2O)_4 \cdot 8H_2O$) [18,19]. MMT is built by stack layers of two tetrahedral silica sheets sandwiching one alumina octahedral sheet: this structure is suitable for being intercalated or exfoliated by different modifiers entering the clay nanogalleries [7,20]. SEP possesses a ribbon-like structure, where two sheets of tetrahedral silica units are linked to a central octahedral sheet of magnesium via oxygen atoms that creates a path of tunnels and channels. These latter can also be entered by selected modifiers [21–23].

The clay modification can be performed exploiting cation exchange, electrostatic interaction, hydrogen bond or hydrophobic/hydrophilic interaction. Furthermore, the modifier absorption depends on the structure, charge and surface of clays and on the experimental conditions adopted for the modification.

The literature reports several examples of EVA embedding different nanoclays, usually ion-exchanged with ammonium quaternary salts: the resulting systems showed increased thermal and thermo-oxidative stability with respect to the unfilled copolymer matrix; besides, they also exhibited an enhanced fire behavior. In particular, Jang and coworkers thoroughly investigated the thermal degradation behavior and the fire retardancy of different thermoplastics (namely EVA, PMMA, PA6, PS, PE, PP, SAN, PAN and ABS) embedding an organo-modified clay at 4 wt.%. It was found that the fire retardancy was strictly related to the occurrence of intermolecular reactions (i.e. inter-chain

aminolysis/acidolysis, radical recombination and hydrogen abstraction) during the degradation [24,25].

Duquesne et al. selected two nanoclays, namely Sodium montmorillonite and Cloisite 30B® in order to prepare nanocomposites with enhanced fire retardant properties. These latter were found to depend on the structure of the clay and its loading; besides, the dispersion at the nano level of the fillers allowed achieving much better fire performances with respect to the micro level [26].

Quite recently, the effectiveness of certain biomacromolecules (namely, some proteins and nucleic acids) as low impact flame retardants for plastics, textiles and foams has been assessed and proven [27–32]. Among the selected FR biomacromolecules, deoxyribonucleic acid (DNA) turned out to be one of the most effective additive: in fact, it is considered as an "all-in-one" intumescent material, since it comprises the three main components of an intumescent system in its structure [29,33]. More specifically, it contains phosphate groups that are capable to produce phosphoric acid, deoxyribose units that behave as a carbon source and as blowing agents and the nitrogen-containing bases (adenine, guanine, cytosine and thymine) that may release ammonia. In addition, the availability of DNA is becoming competitive with those of other chemicals, thanks to the large-scale method recently developed [34]. The effectiveness of low MW DNA from herring sperm as flame retardant for EVA was already demonstrated, either using the biomacromolecule as a surface coating or in bulk via melt-blending [35–37].

The scientific literature reports only few examples of nanoclay modification with selected biomacromolecules; besides, to the best of the authors' knowledge, the exploitation of the so-modified nanofillers has been only marginally devoted to enhance the flame retardant features of the polymer matrix. In particular, montmorillonite was surface-coated by soy protein (SP) that led to intercalation or exfoliation of the substrate [38]. In another research, a monolayer of polydopamine was immobilized onto clay surface and later incorporated into an epoxy resin (3.5 wt.% loading). This resulted in increase of storage modulus up to 30% [39]. The intercalation of cationic chitosan into MMT layers was carried out to obtain compact and robust three-dimensional nanocomposites that, combined with graphite, allowed fabricating bulk-modified electrodes [40]. Then, montmorillonite was modified with quaternized chitosan nanoparticles and embedded into an epoxy-resin [41]. 5 wt.% nanoclay loading enhanced the tensile modulus by about 74%; in addition, a lower loading (i.e. 2.5 wt.%) increased significantly the T_g of the neat resin from 172 °C to 184 °C. The same research group incorporated DNA-modified montmorillonite into an epoxy-resin (2.5 wt.%) and observed an improvement of the flame retardant properties, as well as an increase of the mechanical behavior of the obtained composites [42]. In particular, the peak of heat release rate (PHRR) was decreased by 20.1% and the total heat release (THR) was visibly suppressed by the

presence of intercalated DNA since the value was reduced by 31.2% with respect to the unfilled epoxy-resin. Finally, the tensile strength of the resulting composite was increased by around 20%.

In this work we assess the effect of the presence of DNA-modified clays (namely MMT or SEP) on the fire retardant properties of an EVA copolymer (19% vinyl acetate content). The two selected nanoclays differ as far as the structure is considered: therefore, they are expected, after modification with the biomacromolecule, to affect the fire retardance of EVA in a different way. To the best of the authors' knowledge, this is the first example, in which two different clays, modified with deoxyribonucleic acid strands, are compared as far as their effect on the flame retardance of EVA copolymer is considered. To this aim, the clays were first modified with low MW deoxyribonucleic acid, following a procedure reported in the literature [42]. Then, composites containing 10 wt.% of the DNA-modified clays were obtained by melt compounding in a Brabender mixer: this concentration was selected after different trials using lower or higher modified clay loadings. In particular, loadings below 10 wt.% did not show significant enhancements in the fire behavior of the copolymer, while higher loading made this latter too brittle and therefore unsuitable for functional purposes. The rheological, thermal, mechanical and fire behavior of the resulting composites was thoroughly investigated and compared with that of EVA and composites containing the same amount of unmodified clays. From an overall point of view, the incorporation of the clays, irrespective of the possible modification with DNA, showed a very limited effect on the flammability of the copolymer; however, as assessed in forced combustion tests, the clays, modified or not, lowered both the thermal (i.e. heat release rate and peak of heat release rate) and smoke (namely, total smoke production and specific extinction area) parameters with respect to unfilled EVA. For these latter, the modification of the clays led to better performances as compared to the unmodified counterparts. As expected, the incorporation of the clays (either unmodified or modified with the biomacromolecule) turned out to increase the stiffness of the copolymer, lowering, at the same time, its ductility, without a significant embrittlement.

2 Materials and methods

An ethylene vinyl acetate copolymer, Greenflex® EVA MQ 40F (19% vinyl acetate content) was kindly supplied by Versalis Spa (Mantova, Italy). Montmorillonite clay Sodium Cloisite® and sepiolite were purchased from Southern Clay Products (Gonzales, TX, USA) and TOLSA (Madrid, Spain), respectively.

Deoxyribonucleic acid (DNA) from herring sperm testes (<50bp) and 1M HCl solution were purchased from Sigma Aldrich® (Milano, Italy). Water solutions/suspensions were prepared using 18.2 MΩ deionized water supplied by a Q20 Millipore system (Milano, Italy).

2.1 Modification of Sodium Cloisite with DNA

Briefly, 2g of DNA and 2g of clay were individually dissolved and dispersed respectively in 200ml of deionized water and heated up to 60°C. Afterwards, the DNA solution was adjusted to pH ~2 with HCl and combined with the clay suspension. The resulting mixture was stirred for 20 h and then centrifuged for 60min at 4100rpm. The supernatant was discarded and the precipitated washed two times with deionized water and centrifuged again. The resulting product, hereinafter coded as MMTmod, was dried overnight at 60°C and grounded using a mortar.

2.2 Modification of sepiolite with DNA

Briefly, 3g of sepiolite were suspended in 400ml of water and sonicated for 50min at room temperature. 2g of DNA were dissolved in 100ml of deionized water, the solution was heated up to 60°C; then its pH was adjusted to ~2. Later, the DNA solution and the sepiolite suspension were combined and stirred for 20 h, then centrifuged for 60min. The supernatant was discarded and the precipitated washed two times with deionized water and centrifuged again. The resulting product, hereinafter coded as SEPmod, was dried overnight at 60°C and grounded using a mortar.

2.3 Preparation of EVA-based composites

The different composites were prepared using a Brabender mixing unit, operating at 110°C, working at 80 rpm, for 3 min. The formulations are shown in Table 1.

Table 1. Formulations of the investigated compounds.

Sample code	**Composition (wt.%) of the compounded material**				
	EVA	MMT	MMTmod	SEP	SEPmod
EVA	100				
EVA/MMT	90	10			
EVA/MMTmod	90		10		
EVA/SEP	90			10	
EVA/SEPmod	90				10

3 Characterization techniques

X-ray diffraction spectra were collected on Panalytical X'PERT PRO with copper Cu Kα radiation (λ = 1.54059 Å) in the 2θ range of 2–30° and a step size of 0.026 °/min. All samples were dried at 60°C before XRD measurements.

FT-IR ATR spectra were collected using Perkin-Elmer spectrophotometer (model: Frontier FTIR) equipped a diamond probe. FTIR spectra were recorded at wavelengths from 600 to 4000 cm^{-1}, collecting 16 scans with 4 cm^{-1} resolution.

Rheological analyses were performed using a ARES (TA Instrument Inc., Waters LLC, USA) strain-controlled rheometer in parallel plate geometry (plate diameter: 25 mm). The complex viscosity was measured performing frequency scans from 10^{-1} to 10^{2} rad/s at 110°C. The strain amplitude was fixed at γ = 10%, which is low enough to be in the linear viscoelastic regime, as probed by preliminary strain sweep measurements.

The surface morphology of the composites was investigated using a LEO-1450VP Scanning Electron Microscope (beam voltage: 20kV). Fragments of the compounds obtained by a brittle fracture in liquid nitrogen were fixed to conductive adhesive tapes and gold-metallized.

Thermogravimetric analyses were carried out using a TAQ500 analyzer (TA Instrument Inc., Waters LLC, USA) in the temperature range from 50 to 800°C and with a heating rate of 10°C/min, under nitrogen or air flow of 60 ml/min. Tests were performed placing about 10 mg of sample in alumina pans. $T_{5\%}$ and $T_{50\%}$ (temperature, at which 5 and 50% weight loss occurs, respectively), T_{max} (temperature, at which maximum weight loss rate is observed in dTG curves), residue at T_{max} and residue at 800°C were measured.

Differential scanning calorimetry (DSC) analyses were carried out using a QA1000 TA Instrument apparatus (TA Instrument Inc., Waters LLC, USA). All the experiments were performed under dry N_2 gas (50 mL/min) using samples of around 10 mg in sealed aluminum pans. All the materials were heated up from 30 to 150 °C at 10 °C/min. The crystallinity degree was calculated according to [43].

Flammability tests in vertical configuration were performed according to the UL94 standard.

Forced combustion tests were carried out using Noselab Ats Cone Calorimeter (Nova Milanese, Italy) according to the ISO 5660 standard. In particular, square specimens (10x10x0.3 cm^3) were irradiated with a heat flux of 35 kW/m^2 in horizontal configuration; for each formulation, the test was repeated three times and the results averaged. A standard deviation of 2% was calculated for the following parameters: Time to Ignition (TTI, s), Total Heat Release (THR, MJ/m^2), peak of Heal Release Rate (pkHRR, kW/m^2), Total smoke release (m^2/m^2), Total smoke production (m^2) and Specific extinction area (m^2/kg). All the samples were stored for 2 days in the climatic chamber (23°C, 50% humidity) before test.

Tensile tests were performed on dog-bone (type 5A) specimens using an Instron® 5966 Dynamometer (Norwood, MA, USA). An initial deformation speed of 1mm/min was applied and maintained up to the achievement of 1% of deformation. Then the speed was increased up to 100 mm/min until break. 5 specimens for each investigated system were tested and the results averaged.

4 Results and discussion

4.1 XRD characterization of the clays

Montmorillonite (MMT), due to its smectite structure (2:1), possesses two tetrahedral sheets of silica that are sandwiching an octahedral sheet of alumina [17]. This particular feature allows for a cation exchange or for an intercalation of organic substrate between the layers [44]. DNA-intercalation into montmorillonite silica layers has been already reported in the scientific literature [42].

Natural sepiolite (SEP) possesses a 2:1 layer structure of tetrahedral and octahedral sheets, which create arrangement of tunnels and open channels [21]. Unlike MMT, sepiolite layers are connected via covalent bonds that make them stronger. This means that the DNA can be adsorbed onto the outer surface of the nanofiller and DNA strands may protrude from the gaps [21]. In acidic conditions, new silanol groups are formed on sepiolite: they can interact with DNA via hydrogen bonds, thus further helping the modification of the clay.

The structure of obtained materials were examined through X-ray diffraction technique. The X-ray diffractograms of the raw and modified materials are shown in Figure 1. The diffractogram of pristine clay (MMT) at 8.97° shows reflection of (001) crystalline plane. The layer stacking in phyllosilicate is around 10 Å (Table 2). After modification (MMTmod, red line) the interlayer distance was more than doubled (up to 20.79 Å). This clearly supports the DNA intercalation within the nanoclay layers [42,45]. Furthermore, a broadening of the peak was observed: this finding can be ascribed to the presence of slightly disordered structures within clay tactoids [46]. Besides, some small changes are observed in other peaks, which may indicate some decrease in crystallinity.

Conversely, SEPmod (red line, Figure 1B) does show any change in the diffractogram with respect to pristine SEP (black line): this clearly indicates that natural sepiolite maintained its organized structure after modification with DNA. This finding is in agreement with the scientific literature, where similar results are observed for other organo-modifications of the nanofiller [21,47].

Table 2. X-ray analysis: 2θ values and interlayer space of natural clays and modified materials.

Sample	**2θ angle [°]**	**interlayer distance [Å]**
MMT	8.97	9.84
MMTmod	4.24	20.79
SEP	7.37	11.98
SEPmod	7.47	11.81

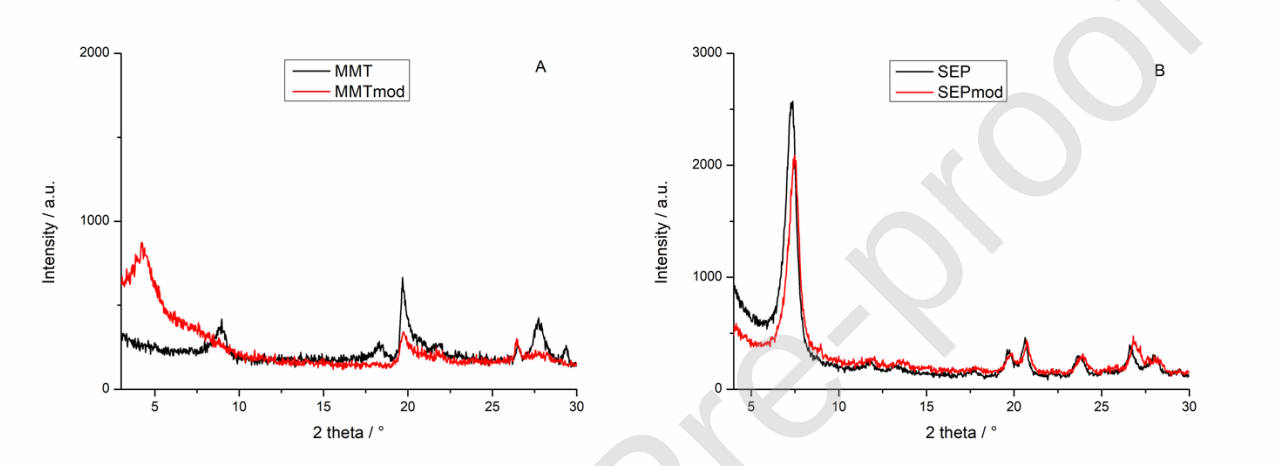

Figure 1. Diffractograms of clays before and after the modification with DNA: A) montmorillonite (MMT) and DNA-modified montmorillonite (MMTmod); B) sepiolite (SEP) and DNA-modified sepiolite (SEPmod).

4.2 FT-IR ATR spectroscopy

Figure 2 shows the FTIR spectra in ATR configuration of the biomacromolecule, as well as of the nanofillers, before and after modification.

As reported in the scientific literature [48,49], the clays display characteristic bands in the region 3670-3600 cm^{-1} (vibrations of Mg-OH of octahedral sheets), broad band between 3450-3400cm^{-1} (presence of water adsorbed on the surface) [50], rather sharp signal at 1640 cm^{-1} (-OH water bending vibrations bands) [51,52] and a very strong signal situated at 1075-1050 cm^{-1} (asymmetric Si-O-Si stretching band). Furthermore, an additional band located around 500 cm^{-1} is attributed to the deformation vibrations of Si–O–Al.

Blue lines in Figures 2A-B display DNA FT-IR ATR spectrum. One can distinguish two bands located at 1230 and 1090 cm^{-1} due to the asymmetric and symmetric stretching of the phosphate groups [48]. The region 1000 – 750 cm^{-1} covers the vibrations bands of the phosphate-sugar backbones. The peak at 1695 cm^{-1} refers to the stretching vibrations of N-H bonds. The broad band between 3400 and 2700 cm^{-1} suggests –OH and –NH overlapping peaks.

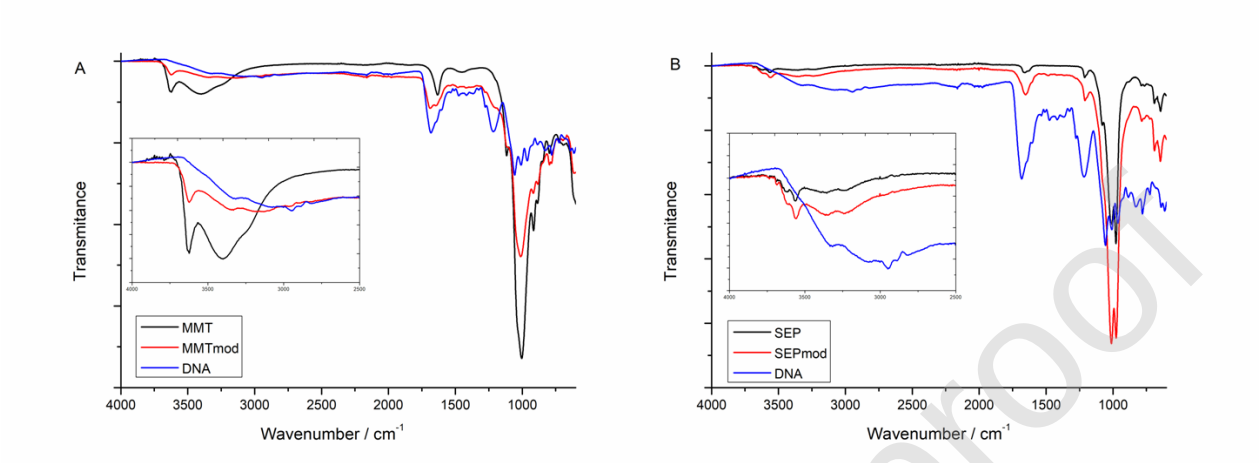

Figure 2. FTIR ATR spectra of DNA and of the nanofillers before and after the modification (Inlet magnifies the bands within 3000 and 3500 cm^{-1}).

In Figure 2A the red line shows montmorillonite intercalated with DNA strands (MMTmod). As a result of the modification, additional peaks at 3300 and 1230 cm^{-1} related to N-H and P-O stretching vibrations of DNA, respectively, appear in the spectrum of MMTmod. Besides, a well visible band at ~1700 cm^{-1} indicates the intercalation of organic substrate, in agreement with previously published data [42].

The spectrum of pristine sepiolite is shown as a black line in Figure 2B. Bands at 3691, 3561 and 3434 cm^{-1} can be assigned to vibrations of Mg-OH, structural water and zeolitic water, respectively [51,52]. The signal located at 1645 cm^{-1} refers to -OH bending of water and the intense wide signal at 1020 cm^{-1} corresponds to Si-O-Si vibrations of tetrahedral units; in addition, the signals at 1220 cm^{-1}, 1087 cm^{-1} and 980 cm^{-1} are attributed to combination bands of Si-O. The spectrum of modified sepiolite (SEPmod, red line, Figure 2B) does not show any significant changes apart from an enrichment and a slight shift of some signals (by 2–5 cm^{-1}), hence further supporting the results from XRD analyses. This finding can also be ascribed to DNA, which shows absorption bands overlapping those of sepiolite. On the other hand, similar slight differences were sufficient to prove the occurrence, after modification, of interactions of aminosilanes [47,51] and an organic dye [52] with sepiolite.

4.3 Thermogravimetric analyses on the nanofillers and DNA

Thermogravimetric analyses in air were carried out on DNA and on the clays, before and after modification with the biomacromolecule, in order to quantitatively assess the modification the clays underwent. The TG and dTG thermograms of DNA, pristine clays and DNA-modified products are shown in Figure 3A-D.

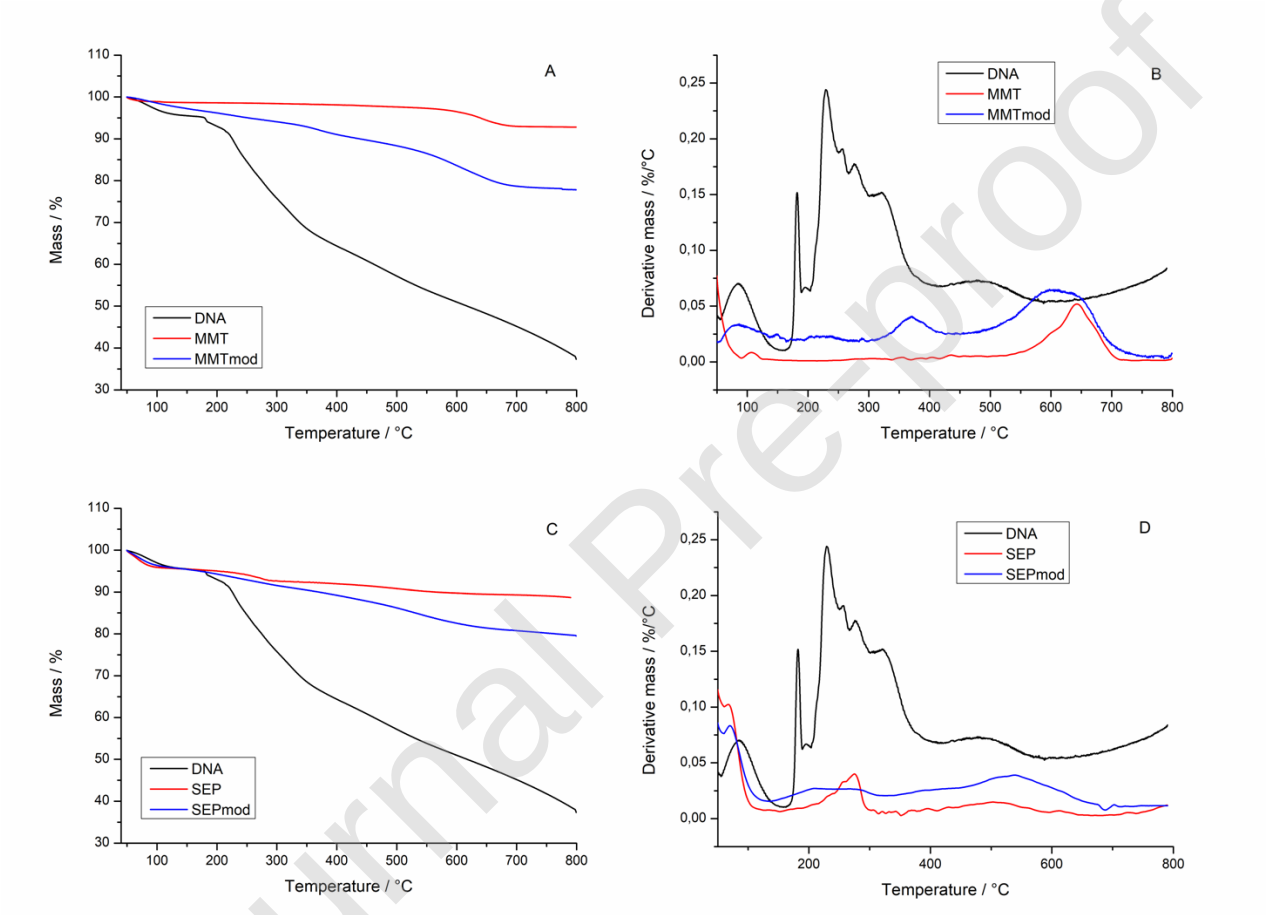

Figure 3. TG and dTG plots of used fillers and DNA in air.

Referring to Figure 3A, one can observe 7.6, 22 and 62.7% mass loss for MMT, MMTmod and DNA, respectively. The difference between the first two mass loss values suggests the presence of 14.4% of DNA within the clay galleries.

TG and dTG curves of DNA in air show significant weight losses at 90°C, in between 182 and 320°C and at 490°C, attributable to loss of water, production of ammonia and degradation of phosphorus groups, respectively.

Pure sepiolite displays four mass loss stages at 64°C (removal of zeolitic water), 275°C, 501°C (both due to loss of coordinated water) and 795°C (because of the occurrence of dehydroxylation reactions) [21]. DNA and sepiolite TG derivative curves (Figure 3D, black and red lines, respectively) overlap in a wide region. However, an intense decomposition step with a maximum at 537°C is observed for SEPmod. As depicted in Figure 3C, SEP and SEPmod show 11.3 and 19.8% mass loss, respectively: therefore, the DNA content onto sepiolite structure was estimated as 8.5%.

The differences in DNA content between MMTmod and SEPmod is not surprising, as the ion exchange capacity for montmorillonite is much higher with respect to sepiolite [53].

4.4 Rheological behavior of the composites

The study of the rheological behavior of polymer-based composites allows gaining an insight into the dispersion of the embedded particles within the host matrix and the interactions established between the two species in the interfacial region. Besides, important information about the material processability can be obtained from the evaluation of the rheological functions in the linear viscoelastic region of the polymer. In Figure 4A-B, the trend of the complex viscosity as a function of frequency for MMT- and SEP-based composites is reported and compared to that of neat EVA. The pure matrix exhibits the typical viscoelastic response of unfilled polymeric materials, with the presence of a Newtonian plateau in the low frequency region, followed by a shear thinning behavior, involving a progressive decrease of the viscosity with increasing of frequency. The presence of MMT particles, irrespective from their possible modification, does not significantly affect the EVA rheological behavior; differently, SEP- and SEPmod-containing composites show higher viscosity values in the whole investigated frequency range, compared to the neat matrix. The obtained results suggest that embedded particles could form some aggregates within the host matrix; however, the presence of these agglomerates does not compromise the processability of the composites, since their viscosity remains quite similar to that of neat EVA in the range of frequency typical of melt-mixing operations.

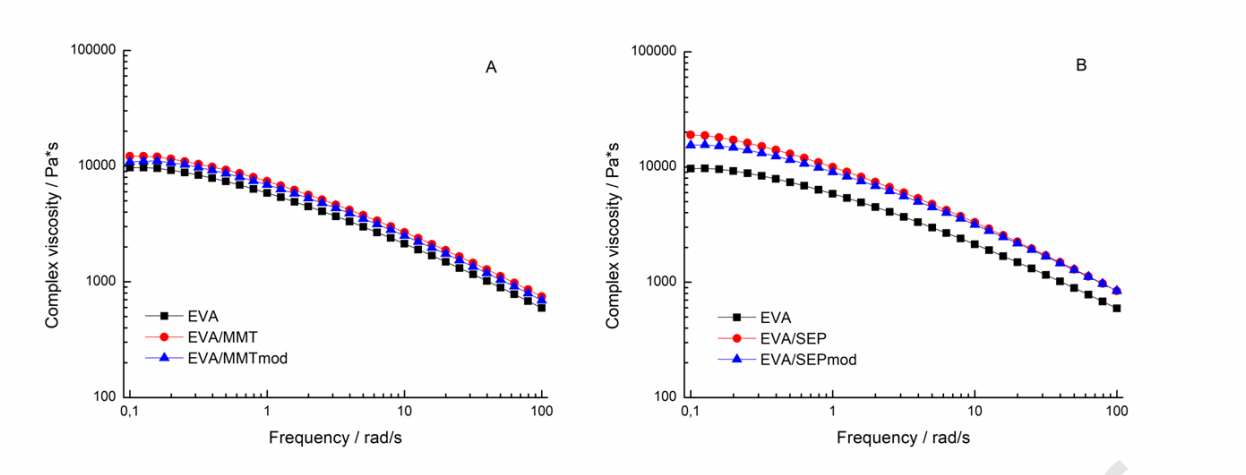

Figure 4. Complex viscosity as a function of frequency for neat EVA and MMT (A) and SEP (B) composites

4.5 Morphology of the prepared composites

SEM analyses were performed on fracture surfaces of the composites, in order to verify the homogeneity of distribution of the fillers before and after the modification with DNA. Some typical images are shown in Figure 5 at different magnifications. Independently from the type of clay and its possible modification, the nanofillers are quite well distributed within the polymer matrix; however, some aggregates, the dimensions of which range from 30 to 150 microns, are formed during the melt compounding process, especially when modified sepiolite is incorporated in EVA.

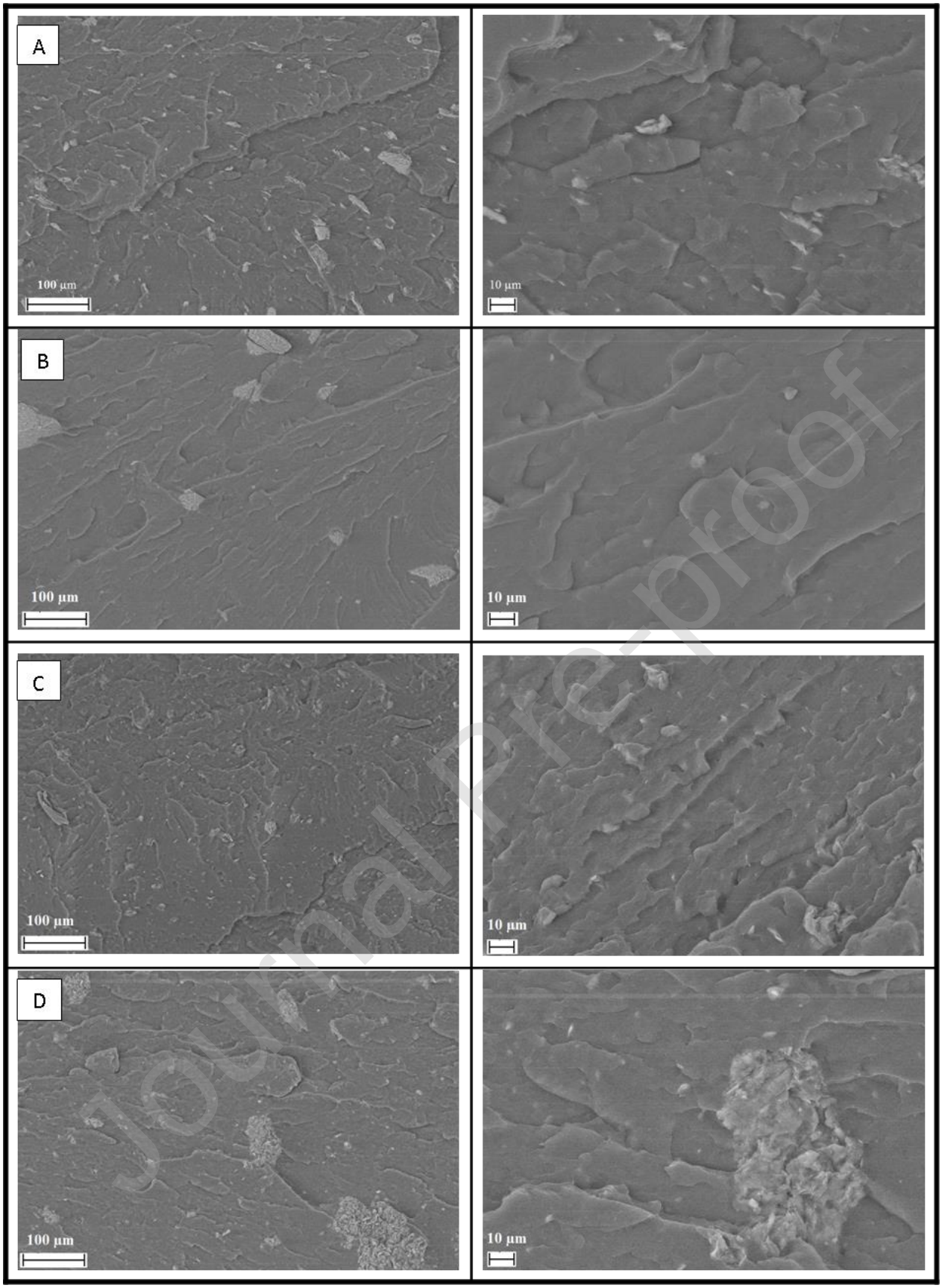

Figure 5. Typical SEM images for the prepared composites at 250 (left panel) and 1000 (right panel) magnifications (line A: EVA/MMT; line B: EVA/MMTmod; line C: EVA/SEP; line D: EVA/SEPmod)

4.6 Thermal and thermo-oxidative stability

The thermal stability of EVA composites was assessed through thermogravimetric analyses (TGA) either in nitrogen or air atmosphere. Figures 6A-D show mass loss and the corresponding derivative (dTG) curves obtained in nitrogen.

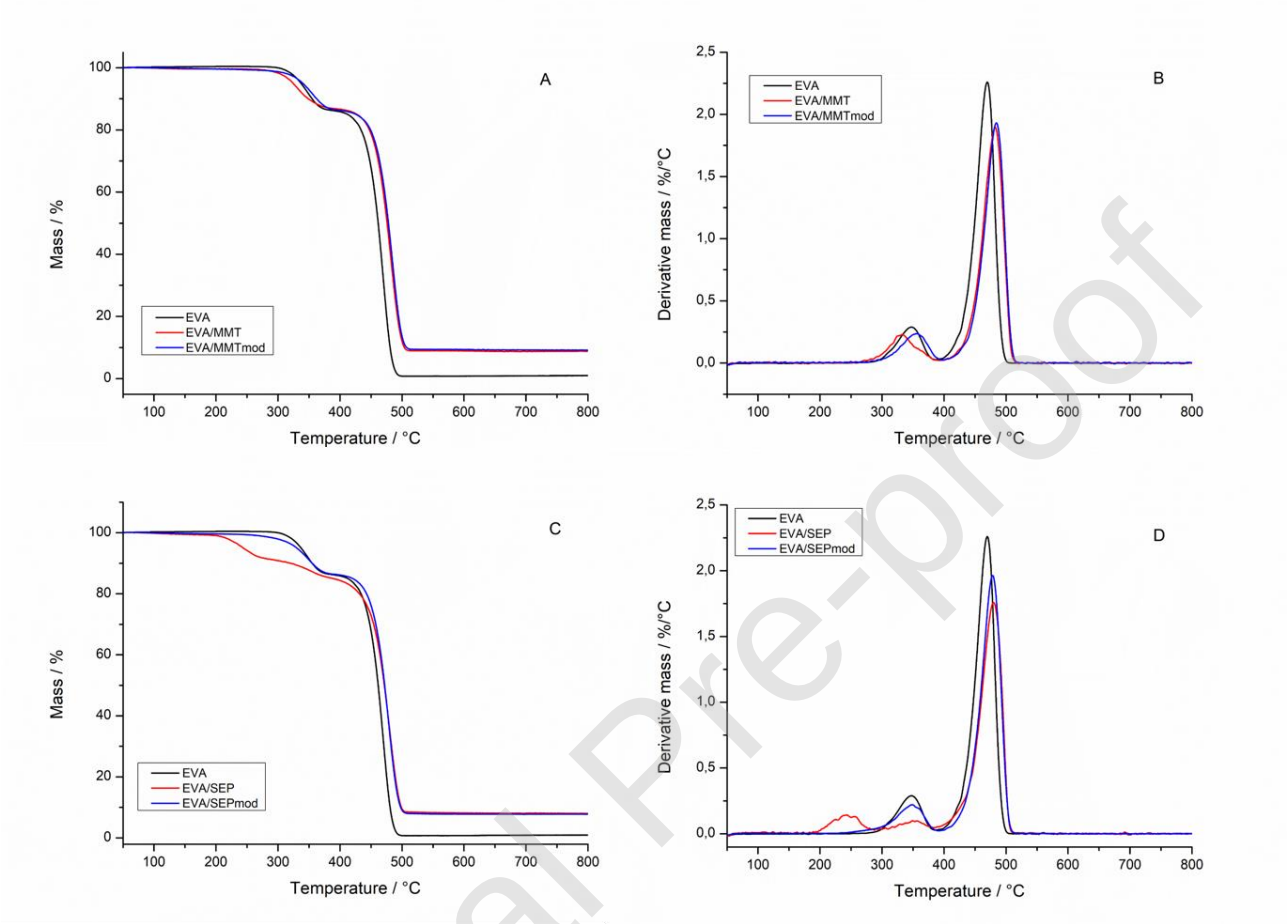

Figure 6. Thermogravimetric curves in nitrogen for clay (A,B) and sepiolite (C,D) composites.

In nitrogen, the thermal decomposition of EVA takes place in two steps [54]. The first one (T_{max1}), occurring between 300 and 395°C, is ascribed to the decomposition of vinyl acetate, and the second one (T_{max2}, between 400 and 500°C), corresponds to the degradation of the polyethylene chains [54]. In all cases, the addition of 10 wt.% of DNA-modified nanofiller, is responsible for an improve of the thermal stability of the copolymer, as shown by the increase of $T_{50\%}$ values collected in Table 3 (478 and 472 vs. 461°C, for EVA/MMTmod, EVA/SEPmod and EVA, respectively). This improvement in the thermal stability may be explained by the physical barrier effect and the entrapment of volatile products arisen from EVA degradation inside the structure of the clays.

More complex changes in the thermogravimetric analyses are observed in air atmosphere (Figure 7). In air, the decomposition of EVA takes place according to three steps. The first two refer

to the loss of acetic acid and the subsequent random chain scission of the remaining material. The third one involves the formation of the char residue [54]. From an overall point of view, the presence of the clays increases the thermo-oxidative stability of the copolymer, as the TG curves of the composites are shifted towards higher temperatures with respect to the unfilled polymer.

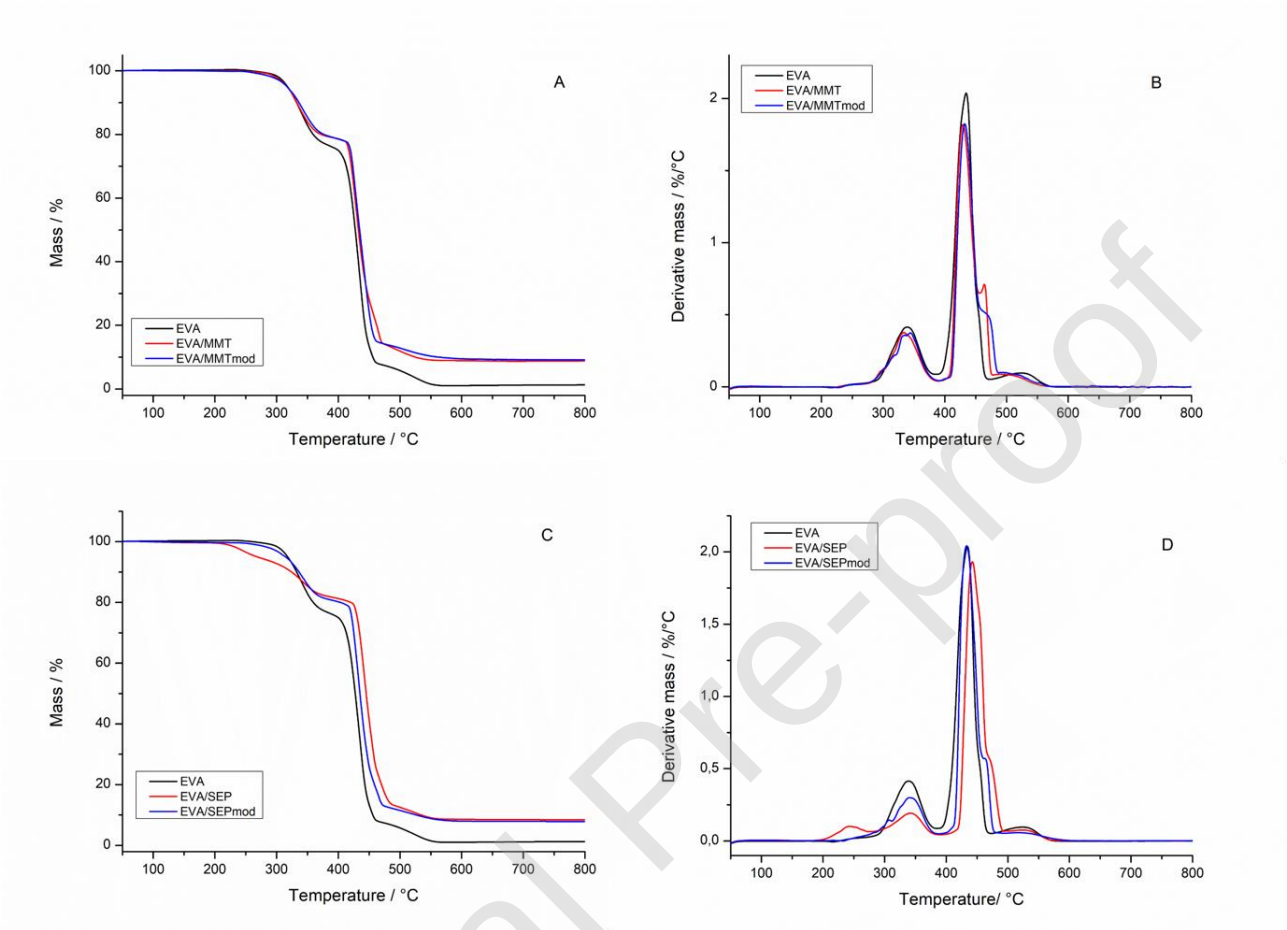

Figure 7. Thermogravimetric curves in air for clay (A,B) and sepiolite (C,D) composites.

As far as EVA/MMTmod is considered, it is worthy to note that the residue in air at 800°C is slightly higher (i.e. 9.1%) with respect to the theoretical one (i.e. 6.6%), calculated on the basis of the composition of the composite. Conversely, there are no significant differences for EVA/SEPmod (7.9 vs. 8%). In fact, as revealed by XRD analyses, the crystalline structure of SEP after the treatment with DNA is not modified at all: this means that DNA is not likely to enter the clay channels, but it's absorbed on the nanofiller surface.

Table 3. The results of thermogravimetric analyses of the obtained composites.

Sample	**$T_{5\%}$ [°C]**	**$T_{50\%}$ [°C]**	**T_{max1} [°C]**	**T_{max2} [°C]**	**T_{max3} [°C]**	**Residue @T_{max1} [%]**	**Residue @T_{max2} [%]**	**Residue @T_{max3} [%]**	**Residue @ 800°C [%]**
Atmosphere: nitrogen									
EVA	328	461	347	470	-	92.2	31.4	-	1.0
EVA/MMT	324	476	332	482	-	93.3	38.6	-	8.8
EVA/MMTmod	340	478	356	484	-	91.5	38.8	-	9.1
EVA/SEP	244	471	354	480	-	87.3	35.5	-	8.0
EVA/SEPmod	330	472	349	479	-	91.3	36.5	-	7.8
Atmosphere: air									
EVA	308	427	339	435	524	87.3	35.1	3.6	0.8
EVA/MMT	317	433	333	429	493	89.9	56.5	12.5	8.8
EVA/MMTmod	317	435	345	432	495	87.1	54.4	13.1	9.1
EVA/SEP	268	445	342	442	525	86.9	56.2	10.7	8.4
EVA/SEPmod	314	435	342	433	525	88.3	54.4	10.1	7.9

4.7 DSC analyses

DSC analyses were exploited in order to assess the effect of the presence of the clays on the degree of crystallinity and T_m of EVA. The results are shown in Figure 8 and Table 4; in particular, the thermograms revealed similar runs for all samples. In a heating range from 30 to 130°C, two endothermal peaks at about 44 and 78°C are observed: as reported in the literature, the former is ascribed to the softening of vinyl acetate parts, while the latter to T_m [55,56]. None of them seems to be remarkably affected by the presence of the fillers, since T_{peak} variations are within 2°C. Conversely, the calculated enthalpies of the second peak suggest a slight decrease in the degree of crystallinity for all the composites with respect to the unfilled polymer matrix. This finding was already reported in the literature for EVA containing bacterial cellulose nanofibers [56].

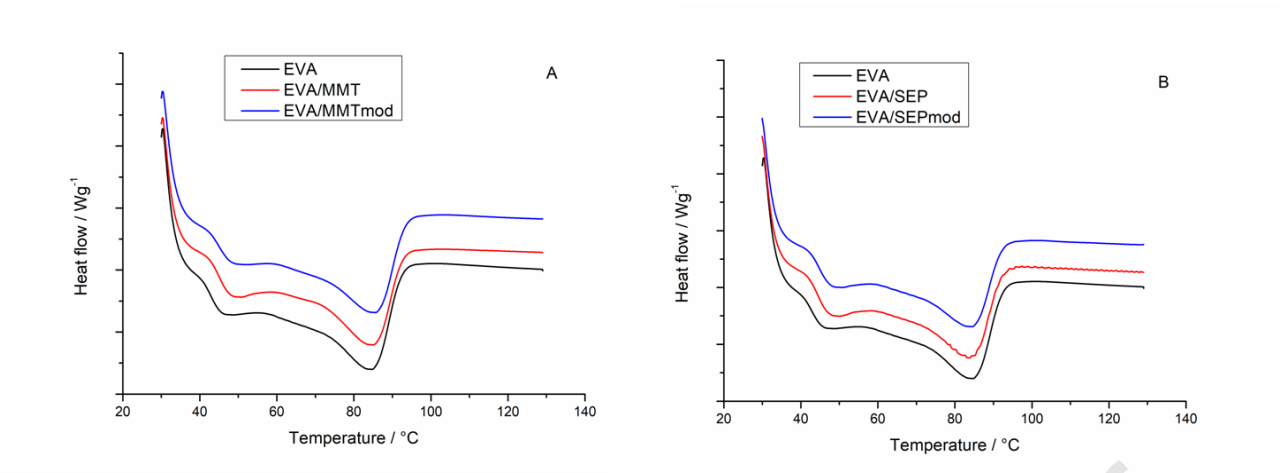

Figure 8. DSC thermograms for A) clay-based and B) sepiolite-based composites.

Table 4. DSC results (endothermal peaks, enthalpy and crystallinity degree) for clay-based and sepiolite-based composites.

Sample	T_{peak1} [°C]	T_{peak2} [°C]	Enthalpy *H* [J/g]	Degree of crystallinity* [%]
EVA	42.7	78.0	27.3	9.4
EVA/MMT	45.1	78.9	22.4	7.7
EVA/MMTmod	45.0	79.5	22.6	7.8
EVA/SEP	44.4	79.0	22.1	7.6
EVA/SEPmod	44.9	78.7	22.1	7.6

*Calculated according to [43]

4.8 Flammability tests

Vertical flame spread tests were performed on EVA and its composites following the UL94 standard. Table 5 collects the obtained data. From an overall point of view, the incorporation of either unmodified or DNA-modified clays in the polymer matrix slightly affects the flammability behavior of the composites: in fact, melt dripping phenomena are not avoided, though, unlike unfilled EVA (no rating), all the composites achieved V2 classification.

Table 5: Results from vertical flame spread tests

Sample	Classification
EVA	-
EVA/MMT	V-2
EVA/MMTmod	V-2
EVA/SEP	V-2
EVA/SEPmod	V-2

4.9 Cone calorimetry tests

Forced combustion tests were carried out in order to study the effect of the clays (before and after modification with DNA) on the resistance to a 35 kW/m^2 irradiative heat flux. Figure 9 shows the HRR vs. time curves; Tables 6 and 7 collect the thermal and smoke parameters, respectively.

First of all, it is noteworthy that the incorporation of any clay in EVA, irrespective of the modification, causes a faster ignition of composites (i.e. a lowering of TTI); the TTI anticipation is more pronounced when the clays were modified with DNA. This behavior can be attributed to the biomacromolecule that has to activate prior the polymer decomposition [57,55].

Furthermore, all the composites, irrespective of the possible modification of the clays with DNA, show a decrease of THR and mean HRR values, as well as a remarkable decrease of pkHRR with respect to unfilled EVA (Table 7). Besides, in any case, the modification of the clays with the biomacromolecule does not provide any improvement in pkHRR values, notwithstanding the slight enhancements of mean HRR and THR values found for EVA/MMTmod composites as compared to EVA/MMT counterparts. Moreover, the modification of sepiolite with DNA leads to lower fire performances with respect to the unmodified clay. This finding could be ascribed to: i) the aggregation phenomena occurring in modified sepiolite when embedded in the polymer matrix and ii) the impossibility of DNA to enter the clay channels, being the former mostly absorbed on the nanofiller surface.

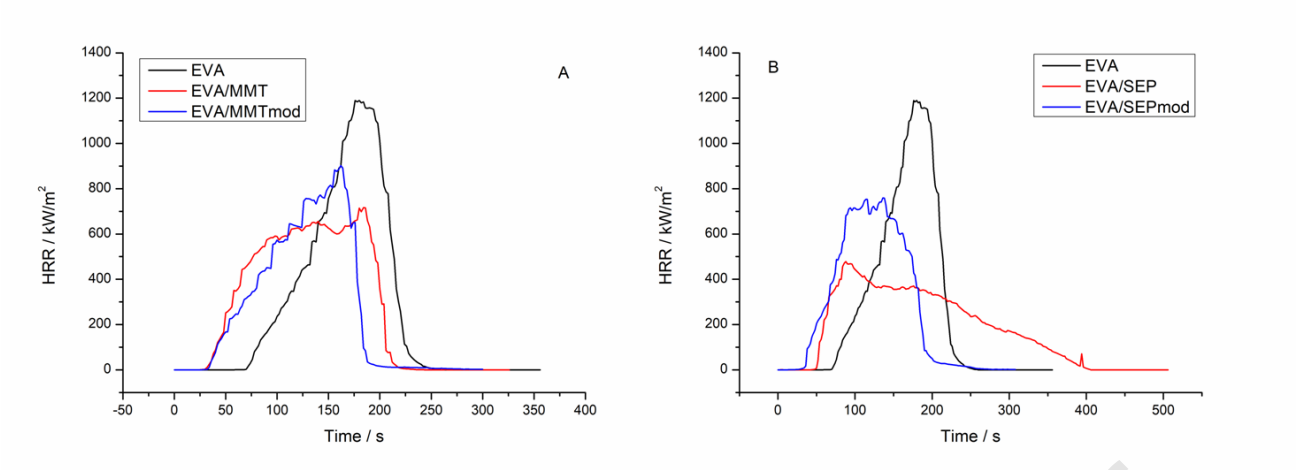

Figure 9. HRR vs. time curves.

Table 6. Cone calorimetry results for EVA and its composites: thermal parameters.

SAMPLE	Time to ignition (s)	mean HRR (kW/m^2)	pkHRR (kW/m^2)	THR (MJ/m^2)	Residue (%)
EVA	69	319	1159	90	0.05
EVA/MMT	37	311	754	89	8.0
EVA/MMTmod	31	298	875	79	6.5
EVA/SEP	48	300	489	81	8.6
EVA/SEPmod	31	294	779	82	7.3

Table 7. Cone calorimetry results for EVA and its composites: smoke parameters.

SAMPLE	TSR (m^2/m^2)	TSP (m^2)	SEA (m^2/kg)	CO yield (kg/kg)	CO_2 yield (kg/kg)
EVA	1543	15.4	608	0.0012	0.0052
EVA/MMT	1752	17.5	702	0.0009	0.0102
EVA/MMTmod	1275	12.8	557	0.0004	0.0084
EVA/SEP	1853	18.6	746	0.0002	0.0052
EVA/SEPmod	1284	12.8	539	0.0015	0.0148

4.10 Mechanical behavior

Finally, tensile tests were carried out on EVA and its composites, aiming at assessing the effect of the fillers on the mechanical behavior of the copolymer. The typical stress-strain curves are shown in Figure 10; Young moduli and elongation at break are collected in Table 8. It is worthy to note that the incorporation of the clays increases the stiffness of the polymer matrix, while decreasing

the ductility (i.e. the elongation at break). These results seem to indicate that 10 wt.% loading (that is much higher as compared to the standard clay content in polymer nanocomposites) does not lead to a significant embrittlement of the copolymer. Besides, the observed mechanical behavior is strictly affected by the micro-size of the modified clays due to the aggregation phenomena already assessed by SEM analyses.

Table 8. Mechanical properties of EVA and its composites.

Sample	**Young Modulus [MPa]**	**Deformation @break [%]**
EVA	13.0 ± 0.6	1227 ± 45
EVA/MMT	17.1 ± 0.6	1064 ± 33
EVA/MMTmod	19.3 ± 0.9	787 ± 102
EVA/SEP	26.9 ± 0.9	908 ± 25
EVA/SEPmod	24.1 ± 1.0	810 ± 65

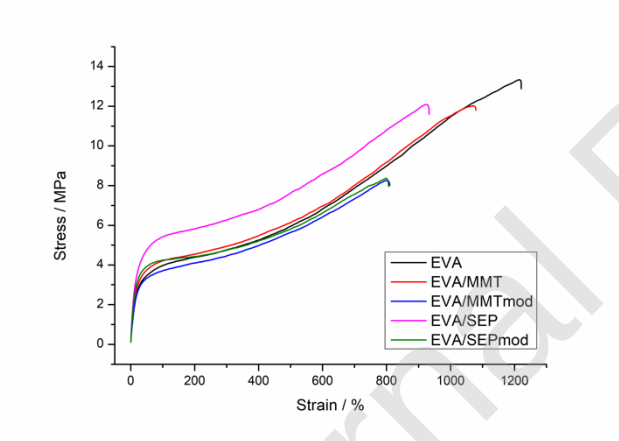

Figure 10. Stress-strain curves for EVA and its composites.

5 Conclusions

Two nanoclays, namely montmorillonite (MMT) and sepiolite (SEP), were modified with low MW DNA strands. The modification was assessed by means of XRD, FT-IR ATR and thermogravimetric analyses. The modified clays were embedded at 10 wt.% loading in EVA copolymer. The obtained composites showed enhanced thermal and thermo-oxidative stability with

respect to unfilled EVA; in addition, the presence of the unmodified or modified fillers slightly reduced the crystallinity degree of the copolymer, without determining significant changes of T_m.

Besides, the presence of the fillers, irrespective of the possible modification, increased the stiffness of the polymer matrix, reducing, at the same time, its ductility. While the flammability of the copolymer was only slightly affected by the presence of the fillers, these latter, as compared to unfilled EVA, turned out to lower the heat release rate (up to 8% for EVA/SEPmod composites), the peak of heat release rate (by 24.5 and 32.8%, respectively for EVA/MMTmod and EVA/SEPmod), the total smoke production (by around 17% for both) and the specific extinction area (between 8 and 11%), as revealed by forced combustion tests.

The control of aggregation seems to be a key issue for the use of the clays modified with DNA at a relevant loading in EVA. Future work will be devoted to enhance the disaggregation/dispersion of the modified clays, in order to further improve the fire behavior and the mechanical properties of the obtained composites.

References

[1] W. Wang, W. Lu, A. Goodwin, H. Wang, P. Yin, N.-G. Kang, K. Hong, J.W. Mays, Recent advances in thermoplastic elastomers from living polymerizations: Macromolecular architectures and supramolecular chemistry, Prog. Polym. Sci. 95 (2019) 1–31. https://doi.org/10.1016/j.progpolymsci.2019.04.002.

[2] A.D. Valino, J.R.C. Dizon, A.H. Espera, Q. Chen, J. Messman, R.C. Advincula, Advances in 3D printing of thermoplastic polymer composites and nanocomposites, Prog. Polym. Sci. 98 (2019) 101162. https://doi.org/10.1016/j.progpolymsci.2019.101162.

[3] H. Kargarzadeh, J. Huang, N. Lin, I. Ahmad, M. Mariano, A. Dufresne, S. Thomas, A. Gałęski, Recent developments in nanocellulose-based biodegradable polymers, thermoplastic polymers, and porous nanocomposites, Prog. Polym. Sci. 87 (2018) 197–227. https://doi.org/10.1016/j.progpolymsci.2018.07.008.

[4] J.-W. Rhim, H.-M. Park, C.-S. Ha, Bio-nanocomposites for food packaging applications, Prog. Polym. Sci. 38 (2013) 1629–1652. https://doi.org/10.1016/j.progpolymsci.2013.05.008.

[5] K. Fueki, C. Ohkubo, M. Yatabe, I. Arakawa, M. Arita, S. Ino, T. Kanamori, Y. Kawai, M. Kawara, O. Komiyama, T. Suzuki, K. Nagata, M. Hosoki, S. Masumi, M. Yamauchi, H. Aita, T. Ono, H. Kondo, K. Tamaki, Y. Matsuka, H. Tsukasaki, M. Fujisawa, K. Baba, K. Koyano, H. Yatani, Clinical application of removable partial dentures using thermoplastic resin. Part II: Material properties and clinical features of non-metal clasp dentures, J. Prosthodont. Res. 58 (2014) 71–84. https://doi.org/10.1016/j.jpor.2014.03.002.

[6] T.R. Hull, R.E. Quinn, I.G. Areri, D.A. Purser, Combustion toxicity of fire retarded EVA, Polym. Degrad. Stab. 77 (2002) 235–242.

[7] T.T. Zhu, C.H. Zhou, F.B. Kabwe, Q.Q. Wu, C.S. Li, J.R. Zhang, Exfoliation of montmorillonite and related properties of clay/polymer nanocomposites, Appl. Clay Sci. 169 (2019) 48–66. https://doi.org/10.1016/j.clay.2018.12.006.

[8] G. Camino, A. Maffezzoli, M. Braglia, M. De Lazzaro, M. Zammarano, Effect of hydroxides and hydroxycarbonate structure on fire retardant effectiveness and mechanical properties in ethylene-vinyl acetate copolymer, Polym. Degrad. Stab. 74 (2001) 457–464.

[9] L. Haurie, A.I. Fernández, J.I. Velasco, J.M. Chimenos, J.-M.L. Cuesta, F. Espiell, Thermal stability and flame retardancy of LDPE/EVA blends filled with synthetic hydromagnesite/aluminium hydroxide/montmorillonite and magnesium hydroxide/aluminium hydroxide/montmorillonite mixtures, Polym. Degrad. Stab. 92 (2007) 1082–1087.

[10] V. Goodarzi, S.H. Jafari, H.A. Khonakdar, S.A. Monemian, M. Mortazavi, An assessment of the role of morphology in thermal/thermo-oxidative degradation mechanism of PP/EVA/clay nanocomposites, Polym. Degrad. Stab. 95 (2010) 859–869.

[11] P. Kiliaris, C.D. Papaspyrides, Polymer/layered silicate (clay) nanocomposites: An overview of flame retardancy, Prog. Polym. Sci. 35 (2010) 902–958. https://doi.org/10.1016/j.progpolymsci.2010.03.001.

[12] F. Laoutid, L. Bonnaud, M. Alexandre, J.-M. Lopez-Cuesta, P. Dubois, New prospects in flame retardant polymer materials: From fundamentals to nanocomposites, Mater. Sci. Eng. R Rep. 63 (2009) 100–125. https://doi.org/10.1016/j.mser.2008.09.002.

[13] W. Zhang, D. Chen, Q. Zhao, Y. Fang, Effects of different kinds of clay and different vinyl acetate content on the morphology and properties of EVA/clay nanocomposites, Polymer. 44 (2003) 7953–7961. https://doi.org/10.1016/j.polymer.2003.10.046.

[14] S. Duquesne, C. Jama, M. Le Bras, R. Delobel, P. Recourt, J.. Gloaguen, Elaboration of EVA–nanoclay systems—characterization, thermal behaviour and fire performance, Compos. Sci. Technol. 63 (2003) 1141–1148. https://doi.org/10.1016/S0266-3538(03)00035-6.

[15] P.S. Khobragade, D.P. Hansora, J.B. Naik, A. Chatterjee, Flame retarding performance of elastomeric nanocomposites: A review, Polym. Degrad. Stab. 130 (2016) 194–244. https://doi.org/10.1016/j.polymdegradstab.2016.06.001.
[16] A. Riva, M. Zanetti, M. Braglia, G. Camino, L. Falqui, Thermal degradation and rheological behaviour of EVA/montmorillonite nanocomposites, Polym. Degrad. Stab. 77 (2002) 299–304.
[17] O. Shepelev, S. Kenig, H. Dodiuk, Nanotechnology Based Thermosets, in: Handb. Thermoset Plast., Elsevier, 2014: pp. 623–695. https://doi.org/10.1016/B978-1-4557-3107-7.00016-6.
[18] A. Esteban-Cubillo, R. Pina-Zapardiel, J.S. Moya, M.F. Barba, C. Pecharromán, The role of magnesium on the stability of crystalline sepiolite structure, J. Eur. Ceram. Soc. 28 (2008) 1763–1768. https://doi.org/10.1016/j.jeurceramsoc.2007.11.022.
[19] A. Alvarez, Sepiolite: properties and uses, in: Dev. Sedimentol., Elsevier, 1984: pp. 253–287.
[20] W.H. Yu, N. Li, D.S. Tong, C.H. Zhou, C.X. (Cynthia) Lin, C.Y. Xu, Adsorption of proteins and nucleic acids on clay minerals and their interactions: A review, Appl. Clay Sci. 80–81 (2013) 443–452. https://doi.org/10.1016/j.clay.2013.06.003.
[21] G. Zhuang, Z. Zhang, H. Chen, Influence of the interaction between surfactants and sepiolite on the rheological properties and thermal stability of organo-sepiolite in oil-based drilling fluids, Microporous Mesoporous Mater. 272 (2018) 143–154. https://doi.org/10.1016/j.micromeso.2018.06.017.
[22] M.A. Moreira, K.J. Ciuffi, V. Rives, M.A. Vicente, R. Trujillano, A. Gil, S.A. Korili, E.H. de Faria, Effect of chemical modification of palygorskite and sepiolite by 3-aminopropyltriethoxisilane on adsorption of cationic and anionic dyes, Appl. Clay Sci. 135 (2017) 394–404. https://doi.org/10.1016/j.clay.2016.10.022.
[23] E.P. Rebitski, A.C.S. Alcântara, M. Darder, R.L. Cansian, L. Gómez-Hortigüela, S.B.C. Pergher, Functional Carboxymethylcellulose/Zein Bionanocomposite Films Based on Neomycin Supported on Sepiolite or Montmorillonite Clays, ACS Omega. 3 (2018) 13538–13550. https://doi.org/10.1021/acsomega.8b01026.
[24] B.N. Jang, M. Costache, C.A.Wilkie, The relationship between thermal degradation behavior of polymer and the fire retardancy of polymer/clay nanocomposites. Polymer 46 (2005) 10678-10687. https://doi.org/10.1016/j.polymer.2005.08.085.
[25] M.C. Costache, D.D. Jiang, C.A.Wilkie, Thermal degradation of ethylene–vinyl acetate coplymer nanocomposites. Polymer 46 (2005) 6947-6958. https://doi.org/10.1016/j.polymer.2005.05.084.
[26] S. Duquesnea, C. Jamaa, M. Le Brasa, R. Delobelb, P. Recourtc, J.M. Gloaguend, Elaboration of EVA–nanoclay systems—characterization, thermal behaviour and fire performance. Comp. Sci. Technol. 63 (2003) 1141–1148. https://doi.org/10.1016/S0266-3538(03)00035-6.
[27] J. Albite-Ortega, S. Sánchez-Valdes, E. Ramirez-Vargas, Y. Nuñez-Figueredo, L.F. Ramos deValle, J.G. Martínez-Colunga, A.Z. Graciano-Verdugo, Z.V. Sanchez-Martínez, A.B. Espinoza-Martínez, J.A. Rodriguez-Gonzalez, M.E. Castañeda-Flores, Influence of keratin and DNA coating on fire retardant magnesium hydroxide dispersion and flammability characteristics of PE/EVA blends, Polym. Degrad. Stab. 165 (2019) 1–11. https://doi.org/10.1016/j.polymdegradstab.2019.03.022.
[28] F. Bosco, A. Casale, C. Mollea, M.E. Terlizzi, G. Gribaudo, J. Alongi, G. Malucelli, DNA coatings on cotton fabrics: Effect of molecular size and pH on flame retardancy, Surf. Coat. Technol. 272 (2015) 86–95. https://doi.org/10.1016/j.surfcoat.2015.04.019.
[29] J. Alongi, R.A. Carletto, A. Di Blasio, F. Carosio, F. Bosco, G. Malucelli, DNA: a novel, green, natural flame retardant and suppressant for cotton, J. Mater. Chem. A. 1 (2013) 4779. https://doi.org/10.1039/c3ta00107e.
[30] Y.-C. Li, Y.-H. Yang, Y.S. Kim, J. Shields, R.D. Davis, DNA-based nanocomposite biocoatings for fire-retarding polyurethane foam, Green Mater. 2 (2014) 144–152. https://doi.org/10.1680/gmat.14.00003.

[31] G. Malucelli, Biomacromolecules and Bio-Sourced Products for the Design of Flame Retarded Fabrics: Current State of the Art and Future Perspectives, Molecules. 24 (2019) 3774. https://doi.org/10.3390/molecules24203774.
[32] M.A.D. Paoli, W.R. Waldman, Bio-based additives for thermoplastics, Polímeros. 29 (2019). https://doi.org/10.1590/0104-1428.06318.
[33] J. Alongi, F. Cuttica, A.D. Blasio, F. Carosio, G. Malucelli, Intumescent features of nucleic acids and proteins, Thermochim. Acta. 591 (2014) 31–39. https://doi.org/10.1016/j.tca.2014.06.020.
[34] L. Wang, J. Yoshida, N. Ogata, S. Sasaki, T. Kajiyama, Self-Assembled Supramolecular Films Derived from Marine Deoxyribonucleic Acid (DNA)−Cationic Surfactant Complexes: Large-Scale Preparation and Optical and Thermal Properties, Chem. Mater. 13 (2001) 1273–1281. https://doi.org/10.1021/cm000869g.
[35] J. Alongi, A.D. Blasio, F. Cuttica, F. Carosio, G. Malucelli, Bulk or surface treatments of ethylene vinyl acetate copolymers with DNA: Investigation on the flame retardant properties, Eur. Polym. J. 51 (2014) 112–119. https://doi.org/10.1016/j.eurpolymj.2013.12.009.
[36] G. Malucelli, M. Barbalini, UV-curable acrylic coatings containing biomacromolecules: A new fire retardant strategy for ethylene-vinyl acetate copolymers, Prog. Org. Coat. 127 (2019) 330–337. https://doi.org/10.1016/j.porgcoat.2018.11.039.
[37] J. Alongi, F. Cuttica, S. Bourbigot, G. Malucelli, Thermal and flame retardant properties of ethylene vinyl acetate copolymers containing deoxyribose nucleic acid or ammonium polyphosphate, J. Therm. Anal. Calorim. 122 (2015) 705–715. https://doi.org/10.1007/s10973-015-4808-5.
[38] M. Jin, Q. Zhong, Structure Modification of Montmorillonite Nanoclay by Surface Coating with Soy Protein, J. Agric. Food Chem. 60 (2012) 11965–11971. https://doi.org/10.1021/jf301934j.
[39] L. Yang, S.L. Phua, J.K.H. Teo, C.L. Toh, S.K. Lau, J. Ma, X. Lu, A Biomimetic Approach to Enhancing Interfacial Interactions: Polydopamine-Coated Clay as Reinforcement for Epoxy Resin, ACS Appl. Mater. Interfaces. 3 (2011) 3026–3032. https://doi.org/10.1021/am200532j.
[40] M. Darder, M. Colilla, E. Ruiz-Hitzky, Biopolymer−Clay Nanocomposites Based on Chitosan Intercalated in Montmorillonite, Chem. Mater. 15 (2003) 3774–3780. https://doi.org/10.1021/cm0343047.
[41] O. Zabihi, M. Ahmadi, M. Naebe, Self-assembly of quaternized chitosan nanoparticles within nanoclay layers for enhancement of interfacial properties in toughened polymer nanocomposites, Mater. Des. 119 (2017) 277–289. https://doi.org/10.1016/j.matdes.2017.01.079.
[42] O. Zabihi, M. Ahmadi, H. Khayyam, M. Naebe, Fish DNA-modified clays: Towards highly flame retardant polymer nanocomposite with improved interfacial and mechanical performance, Sci. Rep. 6 (2016). https://doi.org/10.1038/srep38194.
[43] J. Colombani, A. Sidi, J.-F. Larché, C. Taviot-Gueho, A. Rivaton, Thermooxidative degradation of crosslinked EVA/EPDM copolymers: Impact of Aluminium TriHydrate (ATH) filler incorporation, Polym. Degrad. Stab. 153 (2018) 130–144. https://doi.org/10.1016/j.polymdegradstab.2018.04.005.
[44] T. Okada, Y. Seki, M. Ogawa, Designed Nanostructures of Clay for Controlled Adsorption of Organic Compounds, J. Nanosci. Nanotechnol. 14 (2014) 2121–2134. https://doi.org/10.1166/jnn.2014.8597.
[45] B. Rafiei, F.A. Ghomi, Preparation and characterization of the Cloisite Na+ modified with cationic surfactants, J. Crystallogr. Mineral. 21 (2013) 25–32.
[46] R.A. Vaia, E.P. Giannelis, Polymer melt intercalation in organically-modified layered silicates: model predictions and experiment, Macromolecules. 30 (1997) 8000–8009.
[47] H. Chen, M. Zheng, H. Sun, Q. Jia, Characterization and properties of sepiolite/polyurethane nanocomposites, Mater. Sci. Eng. A. 445–446 (2007) 725–730. https://doi.org/10.1016/j.msea.2006.10.008.

[48] G. Socrates, Infrared and Raman characteristic group frequencies: tables and charts, 3. ed, Wiley, Chichester, 2001.
[49] B. Tyagi, C.D. Chudasama, R.V. Jasra, Determination of structural modification in acid activated montmorillonite clay by FT-IR spectroscopy, Spectrochim. Acta. A. Mol. Biomol. Spectrosc. 64 (2006) 273–278. https://doi.org/10.1016/j.saa.2005.07.018.
[50] E. Chrzanowska, M. Gierszewska, J. Kujawa, A. Raszkowska-Kaczor, W. Kujawski, Development and Characterization of Polyamide-Supported Chitosan Nanocomposite Membranes for Hydrophilic Pervaporation, Polymers. 10 (2018) 868. https://doi.org/10.3390/polym10080868.
[51] S. Ahmed Ben Hassan, D.B. Stojanović, A. Kojović, I. Janković-Častvan, D. Janaćković, P.S. Uskoković, R. Aleksić, Preparation and characterization of poly(vinyl butyral) electrospun nanocomposite fibers reinforced with ultrasonically functionalized sepiolite, Ceram. Int. 40 (2014) 1139–1146. https://doi.org/10.1016/j.ceramint.2013.06.115.
[52] A. Ongen, H.K. Ozcan, E.E. Ozbas, N. Balkaya, Adsorption of Astrazon Blue FGRL onto sepiolite from aqueous solutions, Desalination Water Treat. 40 (2012) 129–136. https://doi.org/10.1080/19443994.2012.671156.
[53] J.M. Huggett, Clay Minerals☆, in: Ref. Module Earth Syst. Environ. Sci., Elsevier, 2015. https://doi.org/10.1016/B978-0-12-409548-9.09519-1.
[54] K. McGarry, J. Zilberman, T.R. Hull, W.D. Woolley, Decomposition and combustion of EVA and LDPE alone and when fire retarded with ATH, Polym. Int. 49 (2000) 1193–1198. https://doi.org/10.1002/1097-0126(200010)49:10<1193::AID-PI537>3.0.CO;2-0.
[55] J.A. Reyes-Labarta, M.M. Olaya, A. Marcilla, DSC and TGA study of the transitions involved in the thermal treatment of binary mixtures of PE and EVA copolymer with a crosslinking agent, Polymer. 47 (2006) 8194–8202. https://doi.org/10.1016/j.polymer.2006.09.054.
[56] S.S. Ghadikolaei, A. Omrani, M. Ehsani, Influences of modified bacterial cellulose nanofibers (BCNs) on structural, thermophysical, optical, and barrier properties of poly ethylene-co-vinyl acetate (EVA) nanocomposite, Int. J. Biol. Macromol. 115 (2018) 266–272. https://doi.org/10.1016/j.ijbiomac.2018.04.071.
[57] M. Karni, D. Zidon, P. Polak, Z. Zalevsky, O. Shefi, Thermal Degradation of DNA, DNA Cell Biol. 32 (2013) 298–301. https://doi.org/10.1089/dna.2013.2056.
[58] F. Carosio, J. Alongi, C. Paravidino, A. Frache, Improving the Flame Retardant Efficiency of Layer by Layer Coatings Containing Deoxyribonucleic Acid by Post-Diffusion of Hydrotalcite Nanoparticles, Materials. 10 (2017) 709. https://doi.org/10.3390/ma10070709.